Table of contents.

1. FIGURES

Figure S1. a) UV Vis spectra of **TPA1PX** versus pH; b) Normalized emission of **TPA1PX** versus pH and c) Molar fraction distribution diagram for protonated species of **TPA1PX** superposed to its normalized emission at 388 nm (λ_{ex} = 314 nm) (●) and the absorbance at 285 nm (●).

Figure S2. a) UV Vis spectra of **TPA2PX** versus pH; b) Normalized emission of **TPA2PX** versus pH and c) Molar fraction distribution diagram for protonated species of **TPA2PX** superposed to its normalized emission at 375 nm (λ_{ex} = 314 nm) (●) and the absorbance at 305 nm (●).

Figure S3. a) UV Vis spectra of **TPA3PX** versus pH; b) Normalized emission of **TPA3PX** versus pH and c) Molar fraction distribution diagram for protonated species of **TPA3PX** superposed to its normalized emission at 375 nm (λ_{ex} = 314 nm) (●) and the absorbance at 305 nm (●).

Figure S4. a) UV Vis spectra of **TPA1P** versus pH; b) Normalized emission of **TPA1P** versus pH and c) Molar fraction distribution diagram for protonated species of **TPA1P** superposed to its normalized emission at 370 nm (λ_{ex} = 314 (●) and the absorbance at 285 nm (●).

Figure S5. a) UV Vis spectra of **TPA2P** versus pH; b) Normalized emission of **TPA2P** versus pH and c) Molar fraction distribution diagram for protonated species of **TPA2P** superposed to its normalized emission at 375 nm (λ_{ex} = 314 (●) and the absorbance at 285 nm (●).

Figure S6. UV/Vis spectra upon increasing **TPA3PX** concentration at pH 12 b) absorbance at 305 nm versus **TPA3PX** concentration at pH 12 and c) emission spectra upon increasing **TPA3PX** concentration at pH 12 (λ_{ex} = 314 nm).

Figure S7. FRET melting curves with 0.2 μM labelled DNA and 1 μM of **TPA-P** ligands: a) HTelo21-K, b) HTelo21-Na, c) 22CTA, d) Bcl-2, e) c-Myc, f) CEB25, g) c-kit1, h) c-kit2 and i) ds26.

Figure S8. FRET melting curves with 0.2 μM labelled DNA and 1 μM of **TPA-PX** ligands: a) HTelo21-K, b) HTelo21-Na, c) 22CTA, d) Bcl-2, e) c-Myc, f) CEB25, g) c-kit1, h) c-kit2 and i) ds26).

Figure S9. Plot of ΔT_m (ºC) for FRET competition assays of **TPA3P**. The values were determined (in triplicate) by conventional FRET melting assays using 0.2 μM of oligonucleotide and 1 μM of the ligand. The equivalents of the duplex competitor (ds26) used are indicated in the plot.

Figure S10. Fluorimetric titration of **TPA3P** with HTelo22-K: a) λ_{ex} = 314 and b) λ_{ex} = 375 nm.

Figure S11. Fluorimetric titration of **TPA3P** with 22CTA: a) λ_{ex} = 314 and b) λ_{ex} = 375 nm.

Figure S12. Fluorimetric titration of **TPA3P** with Bcl-2: a) λ_{ex} = 314 and b) λ_{ex} = 375 nm.

Figure S13. Fluorimetric titration of **TPA3P** with c-Myc: a) λ_{ex} = 314 and b) λ_{ex} = 375 nm.

Figure S14. Fluorimetric titration of **TPA3P** with CEB25: a) λ_{ex} = 314 and b) λ_{ex} = 375 nm.

Figure S15. Fluorimetric titration of **TPA3P** with c-kit1: a) λ_{ex} = 314 and b) λ_{ex} = 375 nm.

Figure S16. Fluorimetric titration of **TPA3P** with c-kit2: a) λ_{ex} = 314 and b) λ_{ex} = 375 nm.

Figure S17. Fluorimetric titration of **TPA2P** with HTelo22-Na: a) λ_{ex} = 314 and b) λ_{ex} = 375 nm.

Figure S18. Fluorimetric titration of **TPA2P** with ds26: a) λ_{ex} = 314 and b) λ_{ex} = 375 nm.

Figure S19. Fluorimetric titration of **TPA1P** with HTelo22-Na: a) λ_{ex} = 314 and b) λ_{ex} = 375 nm.

Figure S20. Fluorimetric titration of **TPA1P** with ds26: a) λ_{ex} = 314 and b) λ_{ex} = 375 nm.

Figure S21. Plot of (Fo-F)/Fo vs DNA concentration for **TPA3P** titrations with different DNA topologies, showing the corresponding fitted curves (a) HTelo22-K, b) HTelo22-Na, c) 22CTA, d) Bcl-2, e) c-Myc, f) CEB25, g) c-kit1, h) c-kit2 and i) ds26).

Figure S22. Plot of (Fo-F)/Fo vs DNA concentration for **TPA2P** titrations with different DNA topologies, showing the corresponding fitted curves (a) HTelo22-K and b) ds26).

Figure S23. Plot of (Fo-F)/Fo vs DNA concentration for **TPA1P** titrations with different DNA topologies, showing the corresponding fitted curves (a) HTelo22-K and b) ds26).

Figure S24. ^{1}H-NMR and ^{13}C-NMR spectra of **TPA1PX** hydrochloride salt in D_2O.

Figure S25. ^{1}H-NMR and ^{13}C-NMR spectra of **TPA2PX** hydrochloride salt in D_2O.

Figure S26. ^{1}H-NMR and ^{13}C-NMR spectra of **TPA3PX** hydrochloride salt in D_2O.

Figure S27. ^{1}H-NMR and ^{13}C-NMR spectra of **TPA1P** hydrochloride salt in D_2O.

Figure S28. ^{1}H-NMR and ^{13}C-NMR spectra of **TPA2P** hydrochloride salt in D_2O.

Figure S29. ^{1}H-NMR and ^{13}C-NMR spectra of **TPA3P** hydrochloride salt in D_2O.

Figure S30. Top view of the minimum energy conformers for de interaction between a) **TPA3P** or b) **TPA3PY** with the G4 DNA model.

2. Tables

Table S.1. Logarithms of the stepwise protonation constants of the three **TPA-P** ligands determined by potentiometric titrations.[a-c]

Table S.2. Logarithms of the stepwise protonation constants of the three **TPA-P** ligands determined by potentiometric titrations.[a-c]

Table S3. ΔT_m values [ºC] for the interaction between different DNA topologies (0.2 μM) and the **TPA-PX** derivatives.

Table S4. ΔT_m values [ºC] for the interaction between different DNA topologies (0.2 μM) and the **TPA-P** derivatives.

Table S5. ΔT_m values [ºC] for the interaction between different DNA topologies (0.2 μM) and the **TPA-PY** derivatives.

3. References

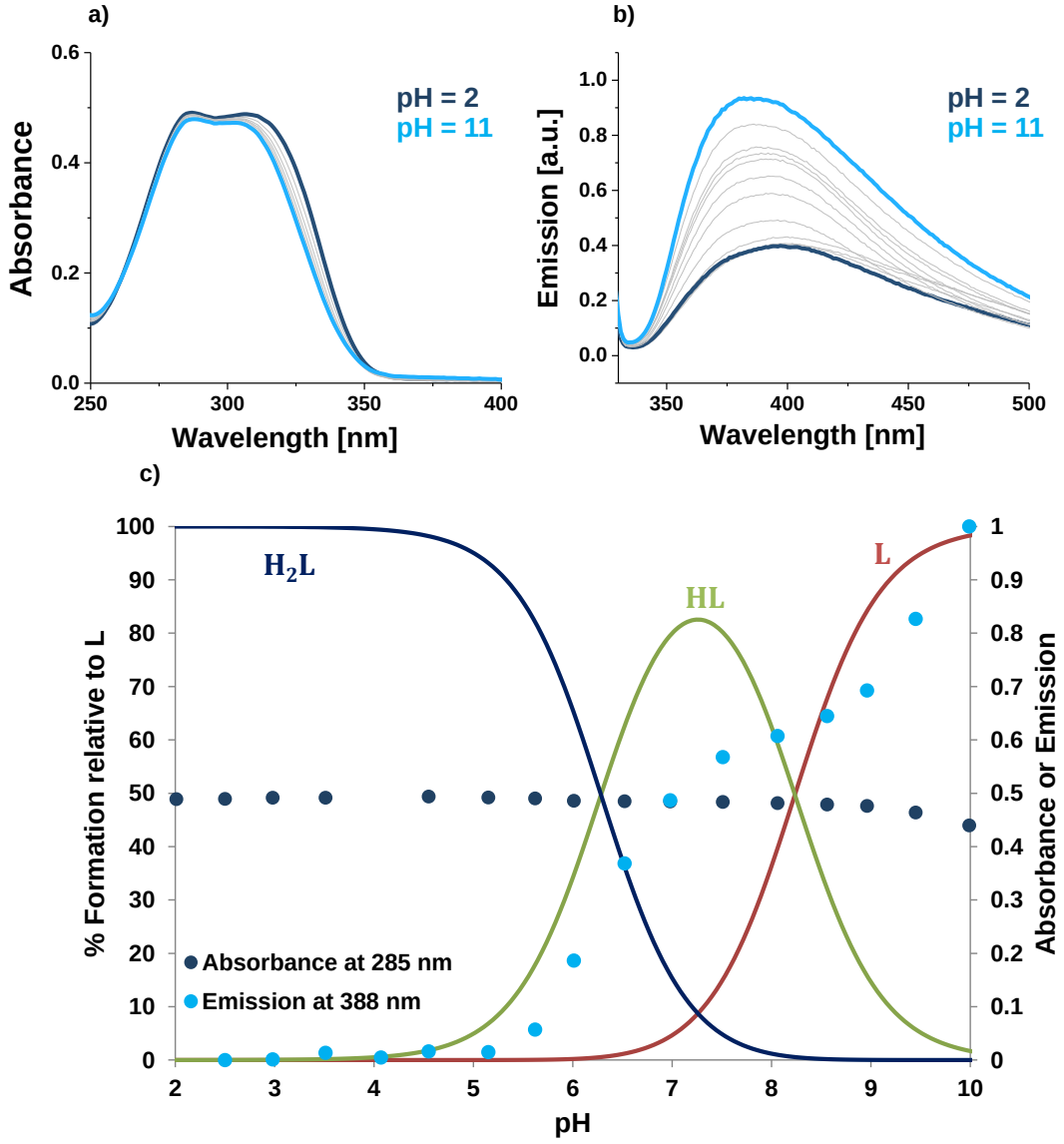

Figure S1. a) UV Vis spectra of **TPA1PX** versus pH; b) Normalized emission of **TPA1PX** versus pH and c) Molar fraction distribution diagram for protonated species of **TPA1PX** superposed to its normalized emission at 388 nm (λ_{ex} = 314 nm) (●) and the absorbance at 285 nm (●).

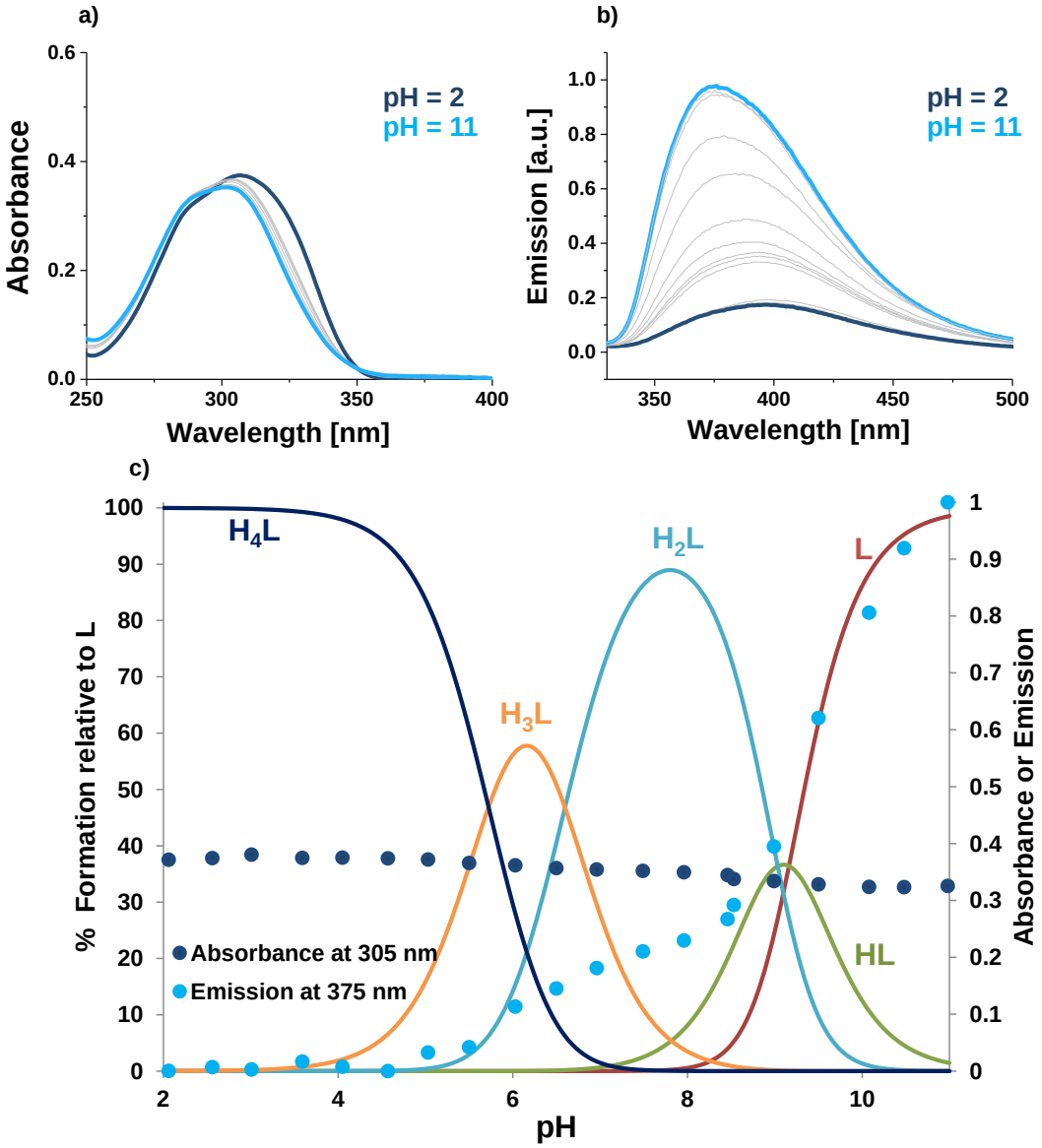

Figure S2. a) UV Vis spectra of **TPA2PX** versus pH; b) Normalized emission of **TPA2PX** versus pH and c) Molar fraction distribution diagram for protonated species of **TPA2PX** superposed to its normalized emission at 375 nm (λ_{ex} = 314 nm) (●) and the absorbance at 305 nm (●).

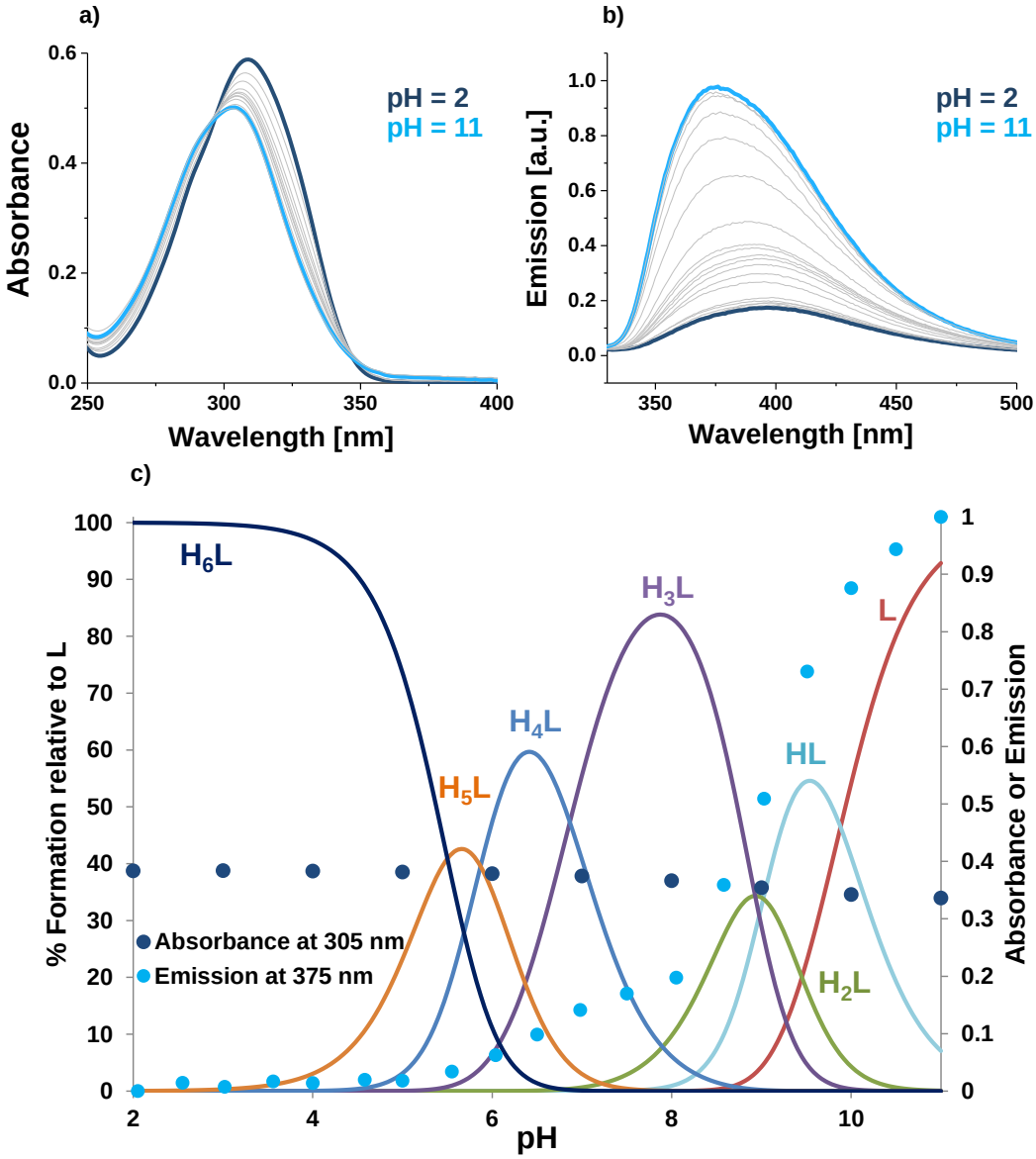

Figure S3. a) UV Vis spectra of **TPA3PX** versus pH; b) Normalized emission of **TPA3PX** versus pH and c) Molar fraction distribution diagram for protonated species of **TPA3PX** superposed to its normalized emission at 375 nm (λ_{ex} = 314 nm) (●) and the absorbance at 305 nm (●).

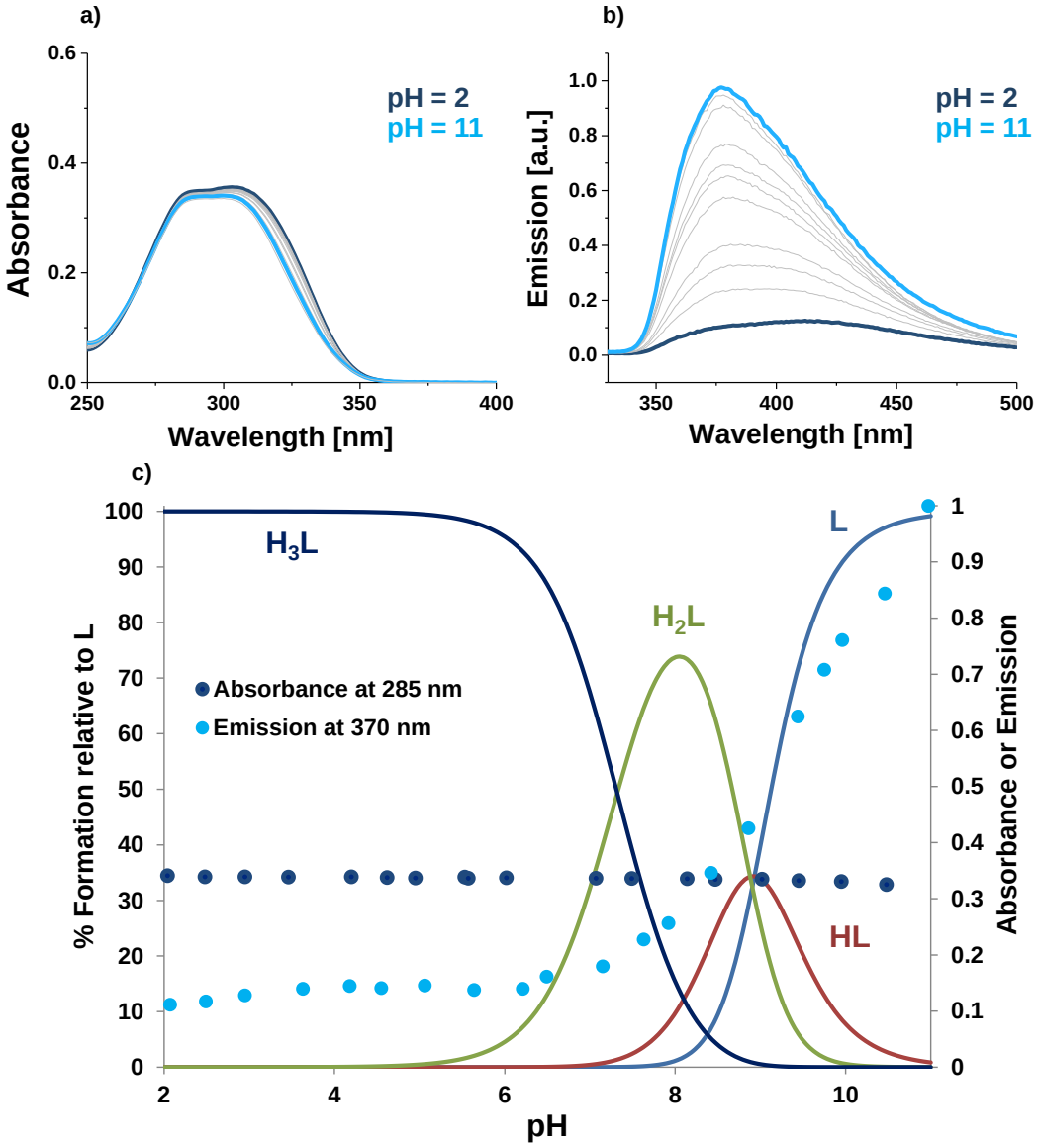

Figure S4. a) UV Vis spectra of **TPA1P** versus pH; b) Normalized emission of **TPA1P** versus pH and c) Molar fraction distribution diagram for protonated species of **TPA1P** superposed to its normalized emission at 370 nm (λ_{ex} = 314 (●) and the absorbance at 285 nm (●).

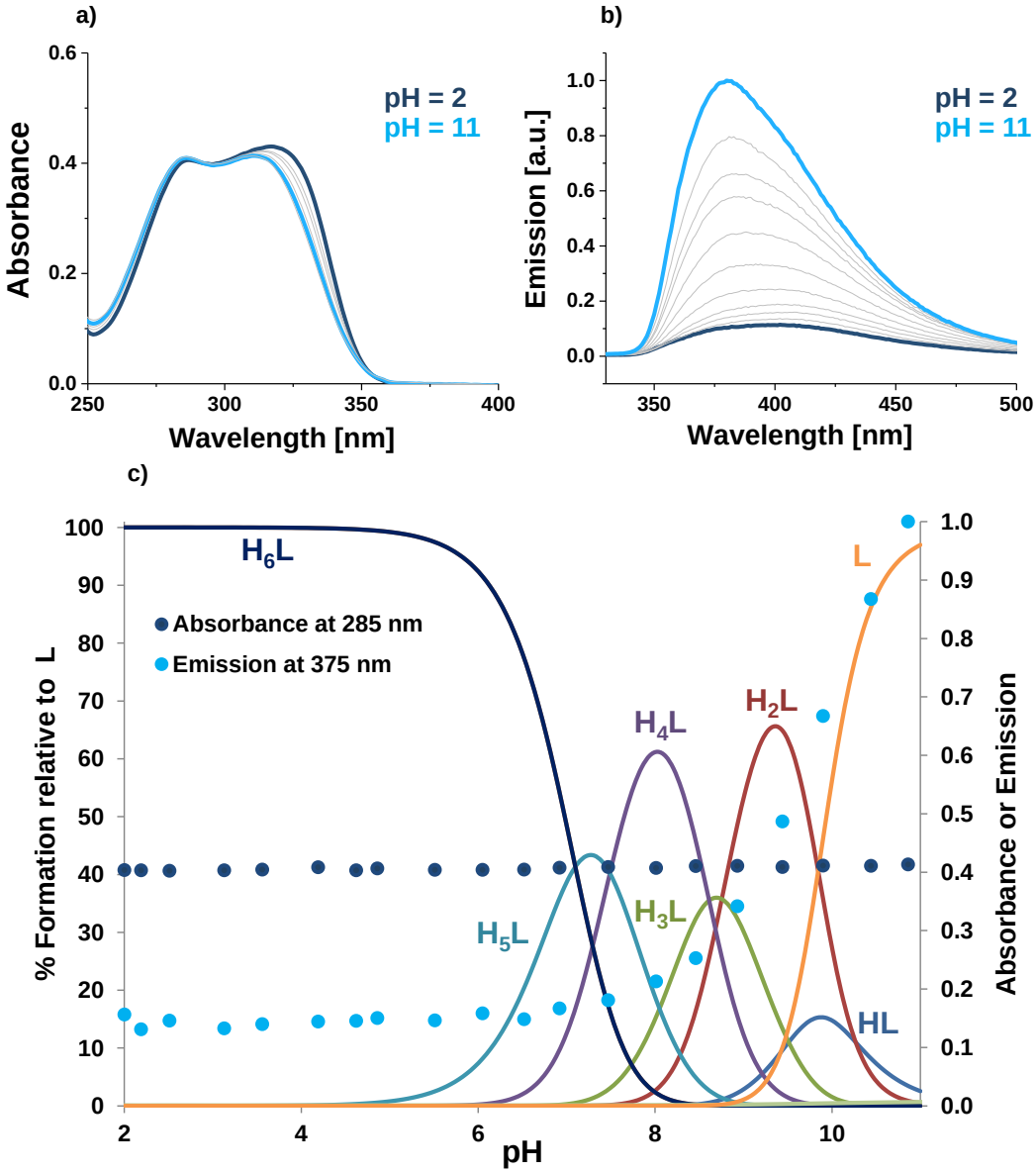

Figure S5. a) UV Vis spectra of **TPA2P** versus pH; b) Normalized emission of **TPA2P** versus pH and c) Molar fraction distribution diagram for protonated species of **TPA2P** superposed to its normalized emission at 375 nm (λ_{ex} = 314 (●) and the absorbance at 285 nm (●).

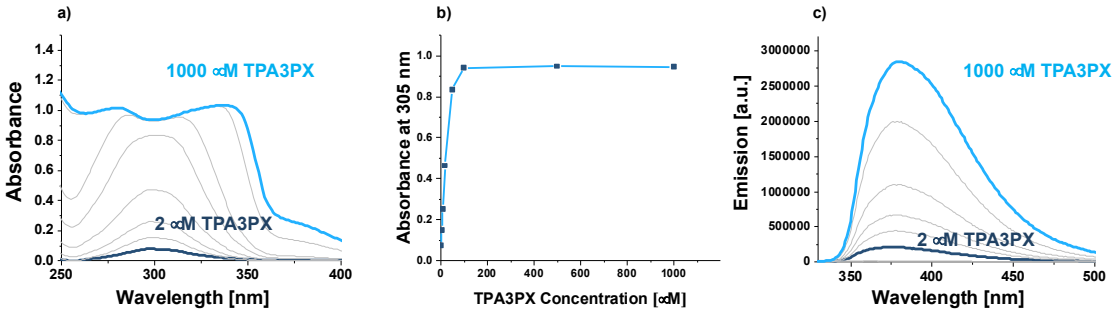

Figure S6. UV/Vis spectra upon increasing **TPA3PX** concentration at pH 12 b) absorbance at 305 nm versus **TPA3PX** concentration at pH 12 and c) emission spectra upon increasing **TPA3PX** concentration at pH 12 (λ_{ex} = 314 nm).

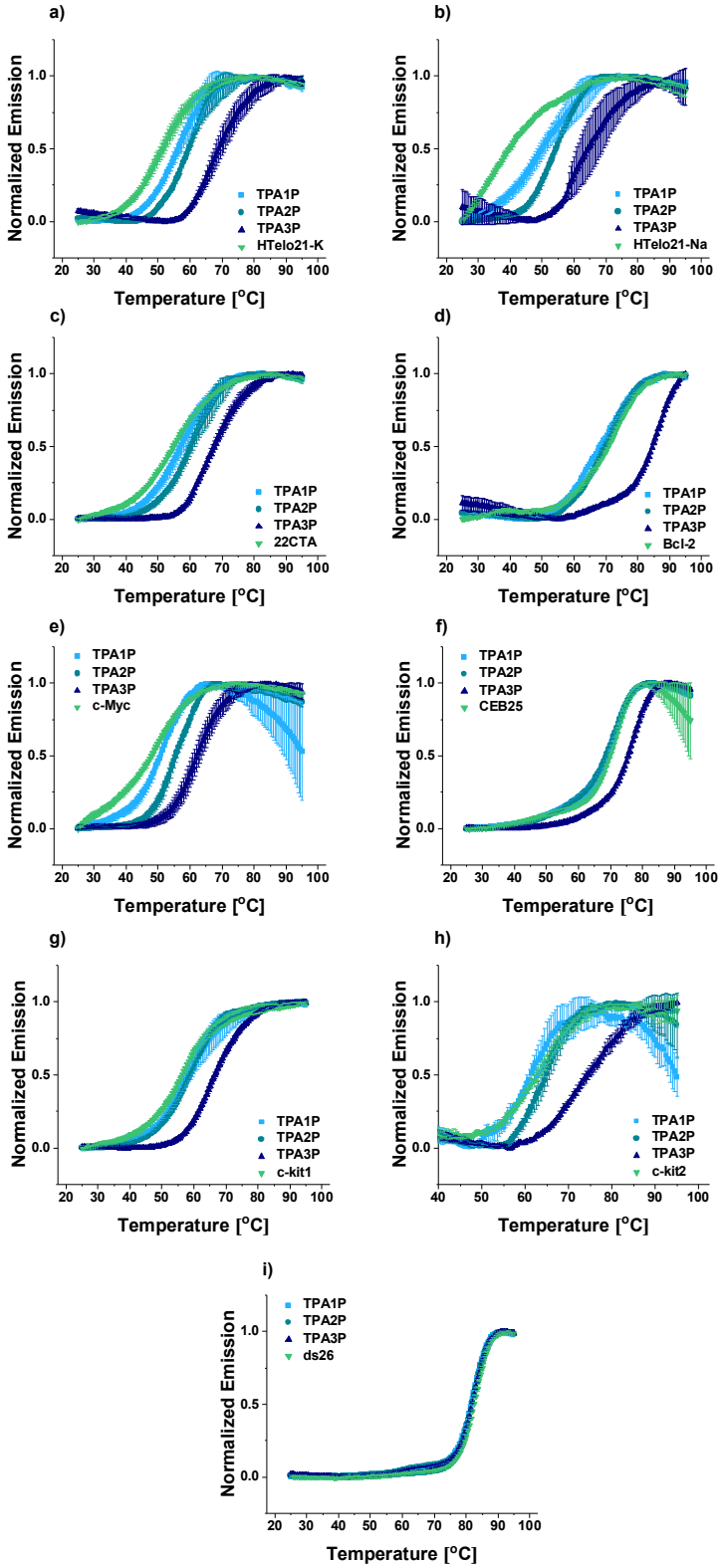

Figure S7. FRET melting curves with 0.2 μM labelled DNA and 1 μM of **TPA-P** ligands: a) HTelo21-K, b) HTelo21-Na, c) 22CTA, d) Bcl-2, e) c-Myc, f) CEB25, g) c-kit1, h) c-kit2 and i) ds26.

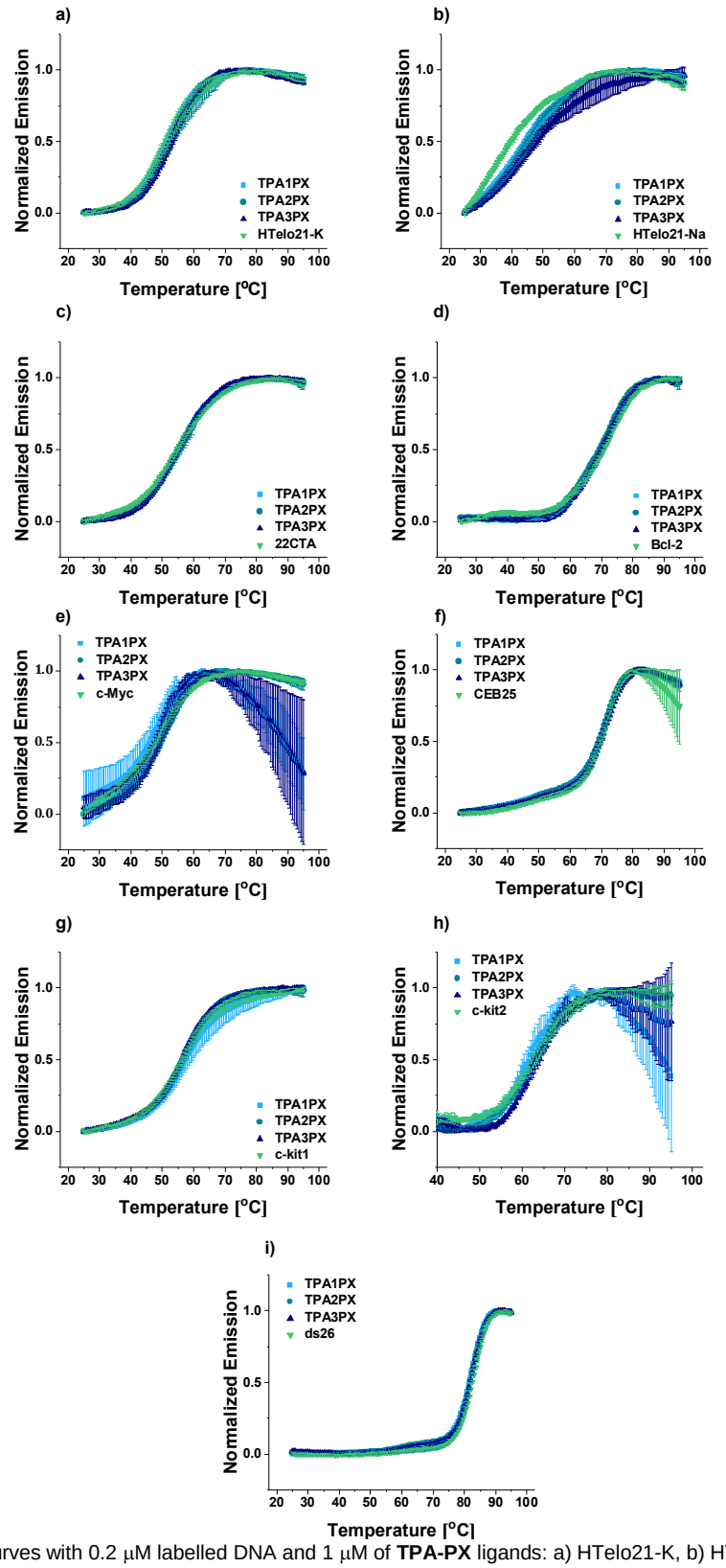

Figure S8. FRET melting curves with 0.2 μM labelled DNA and 1 μM of **TPA-PX** ligands: a) HTelo21-K, b) HTelo21-Na, c) 22CTA, d) Bcl-2, e) c-Myc, f) CEB25, g) c-kit1, h) c-kit2 and i) ds26).

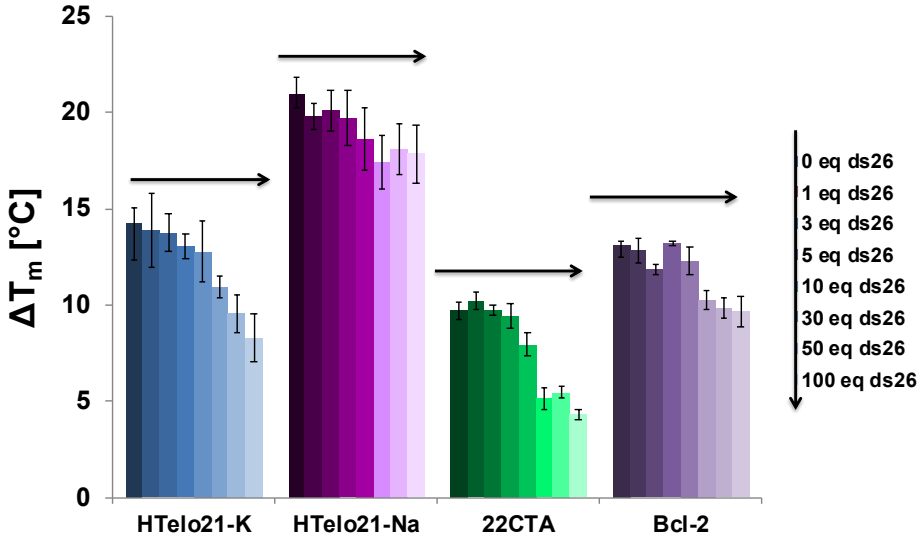

Figure S9. Plot of ΔT_m (ºC) for FRET competition assays of **TPA3P**. The values were determined (in triplicate) by conventional FRET melting assays using 0.2 μM of oligonucleotide and 1 μM of the ligand. The equivalents of the duplex competitor (ds26) used are indicated in the plot.

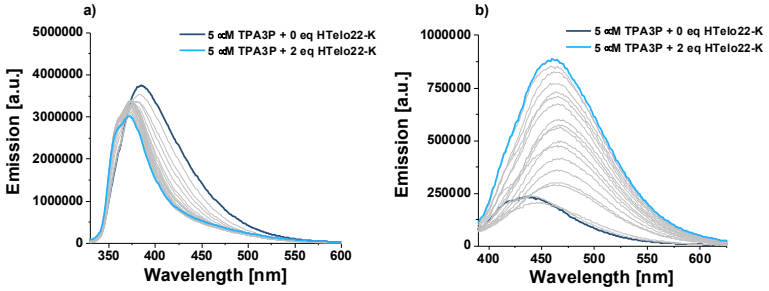

Figure S10. Fluorimetric titration of **TPA3P** with HTelo22-K: a) λ_{ex} = 314 and b) λ_{ex} = 375 nm.

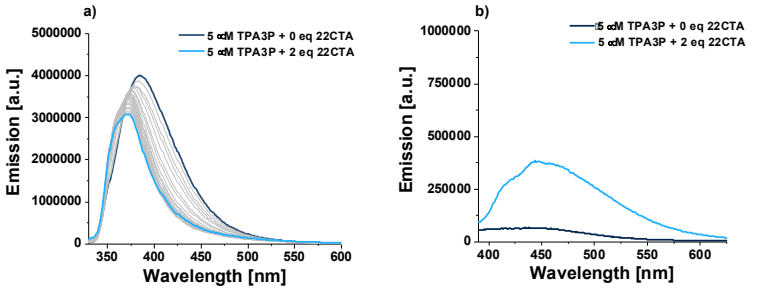

Figure S11. Fluorimetric titration of **TPA3P** with 22CTA: a) λ_{ex} = 314 and b) λ_{ex} = 375 nm.

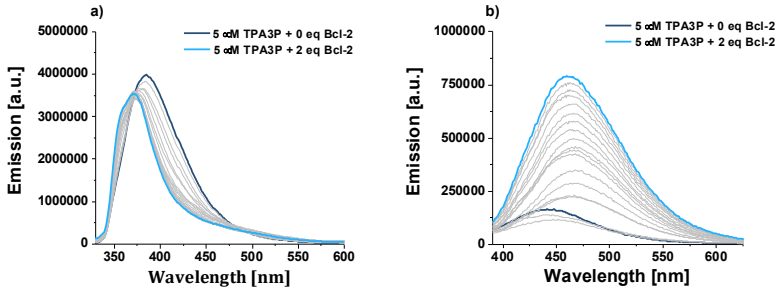

Figure S12. Fluorimetric titration of **TPA3P** with Bcl-2: a) λ_{ex} = 314 and b) λ_{ex} = 375 nm.

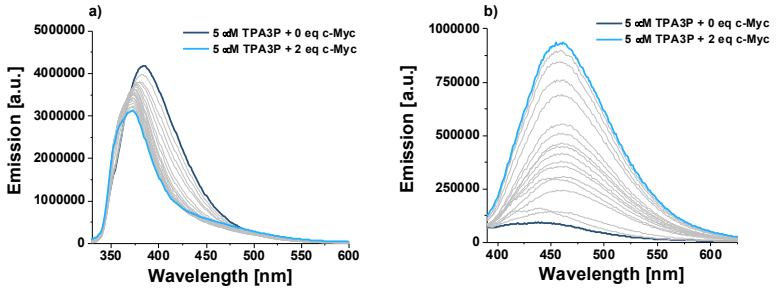

Figure S13. Fluorimetric titration of **TPA3P** with c-Myc: a) λ_{ex} = 314 and b) λ_{ex} = 375 nm.

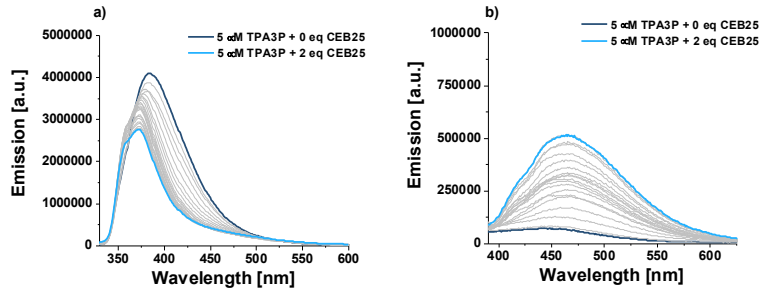

Figure S14. Fluorimetric titration of **TPA3P** with CEB25: a) λ_{ex} = 314 and b) λ_{ex} = 375 nm.

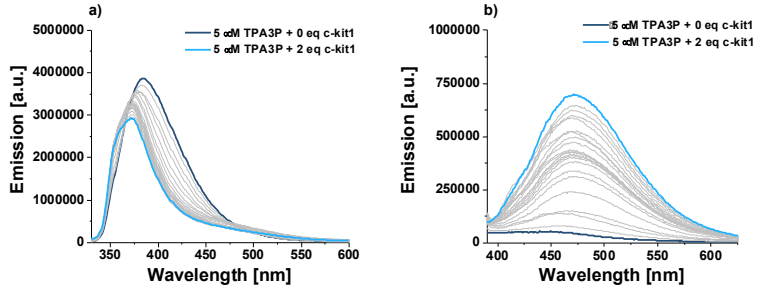

Figure S15. Fluorimetric titration of **TPA3P** with c-kit1: a) λ_{ex} = 314 and b) λ_{ex} = 375 nm.

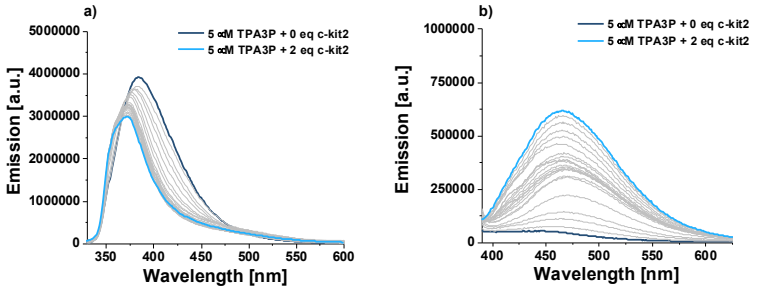

Figure S16. Fluorimetric titration of **TPA3P** with c-kit2: a) λ_{ex} = 314 and b) λ_{ex} = 375 nm.

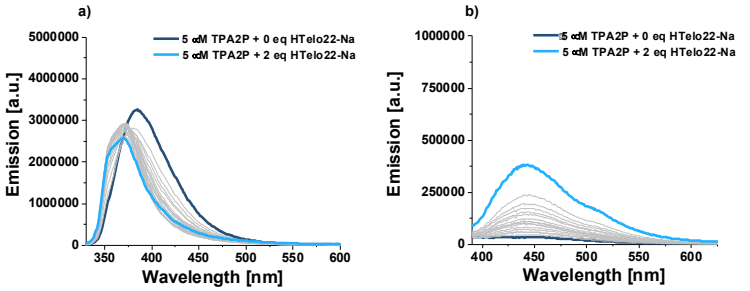

Figure S17. Fluorimetric titration of **TPA2P** with HTelo22-Na: a) λ_{ex} = 314 and b) λ_{ex} = 375 nm.

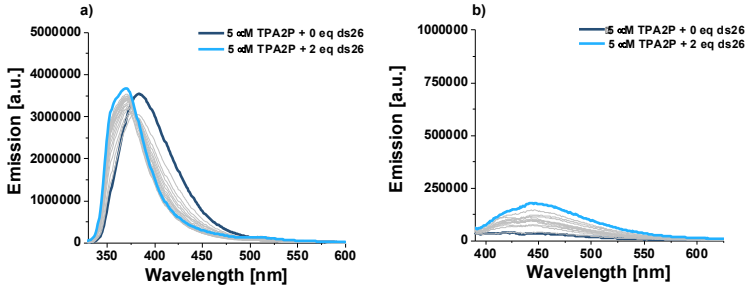

Figure S18. Fluorimetric titration of **TPA2P** with ds26: a) λ_{ex} = 314 and b) λ_{ex} = 375 nm.

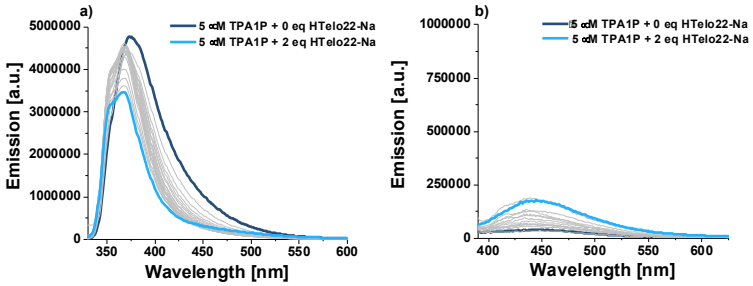

Figure S19. Fluorimetric titration of **TPA1P** with HTelo22-Na: a) λ_{ex} = 314 and b) λ_{ex} = 375 nm.

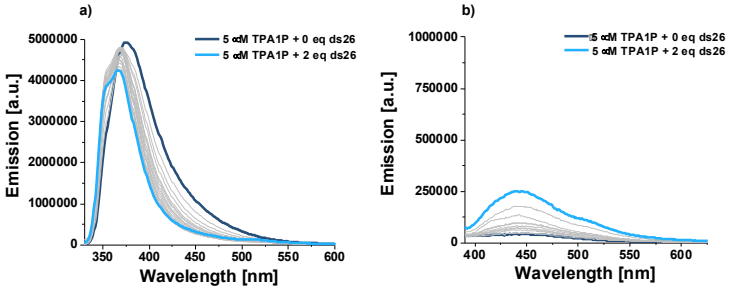

Figure S20. Fluorimetric titration of **TPA1P** with ds26: a) λ_{ex} = 314 and b) λ_{ex} = 375 nm.

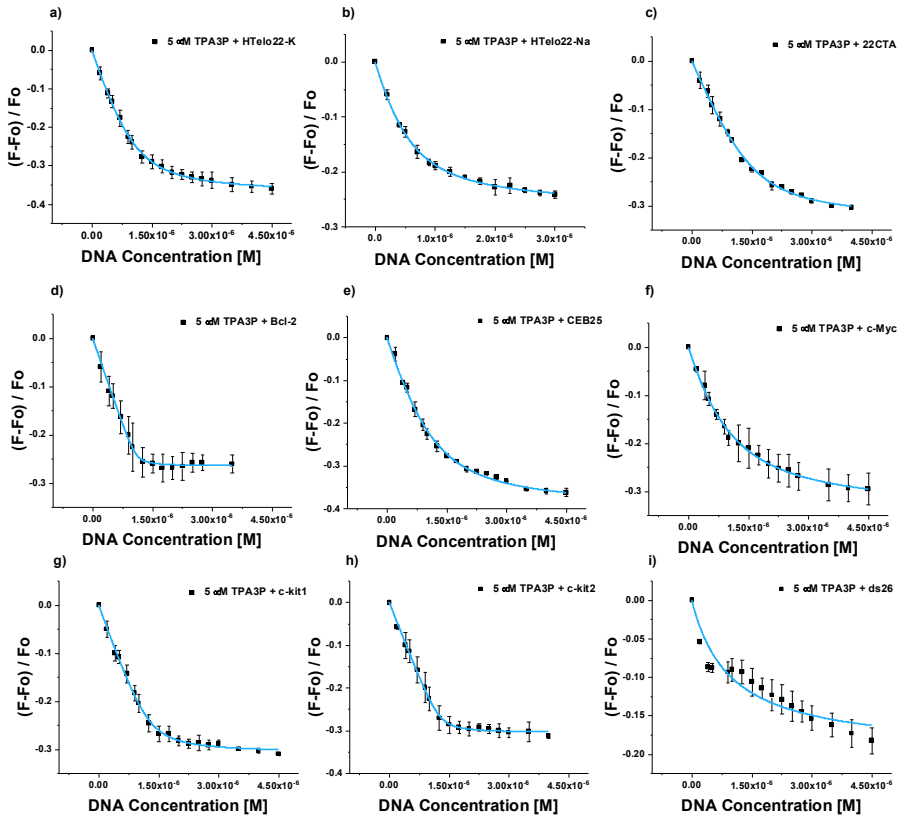

Figure S21. Plot of (Fo-F)/Fo vs DNA concentration for **TPA3P** titrations with different DNA topologies, showing the corresponding fitted curves (a) HTelo22-K, b) HTelo22-Na, c) 22CTA, d) Bcl-2, e) c-Myc, f) CEB25, g) c-kit1, h) c-kit2 and i) ds26).

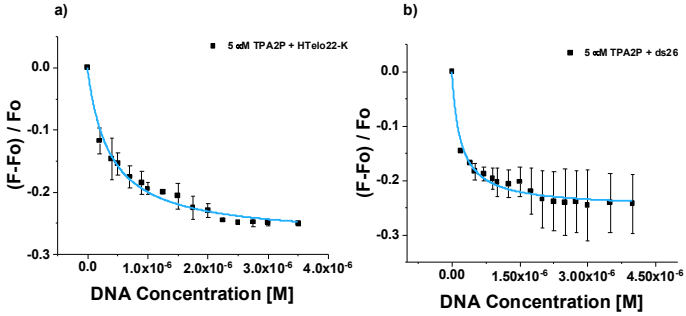

Figure S22. Plot of (Fo-F)/Fo vs DNA concentration for **TPA2P** titrations with different DNA topologies, showing the corresponding fitted curves (a) HTelo22-K and b) ds26).

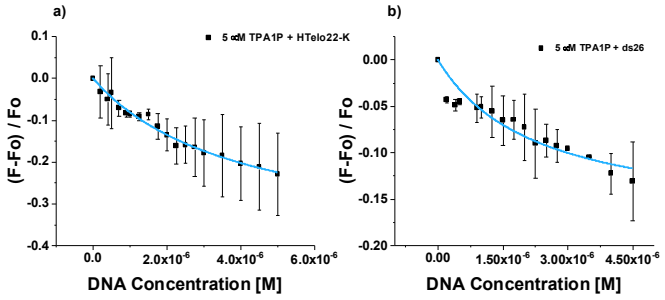

Figure S23. Plot of (Fo-F)/Fo vs DNA concentration for **TPA1P** titrations with different DNA topologies, showing the corresponding fitted curves (a) HTelo22-K and b) ds26).

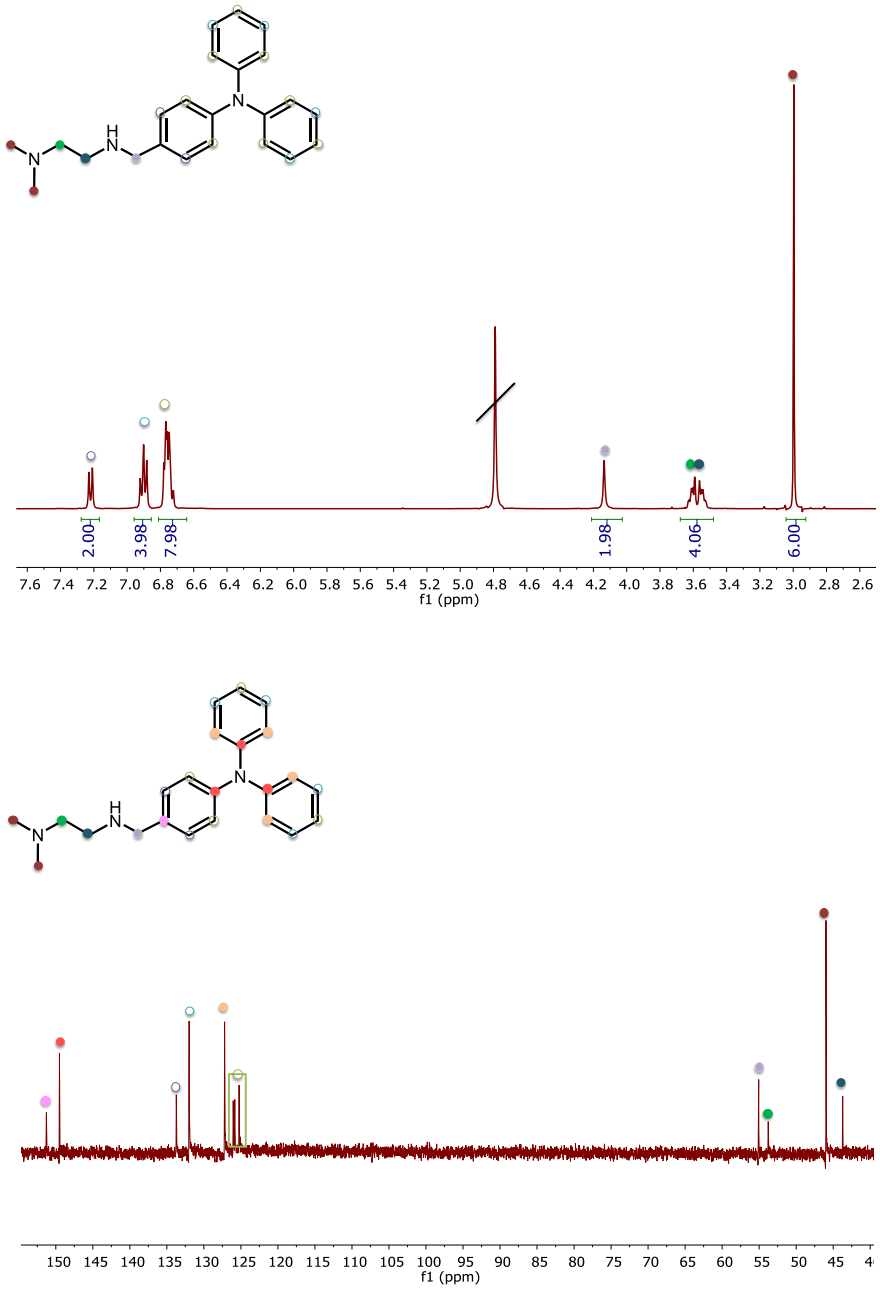

Figure S24. ^{1}H-NMR and ^{13}C-NMR spectra of **TPA1PX** hydrochloride salt in D_2O.

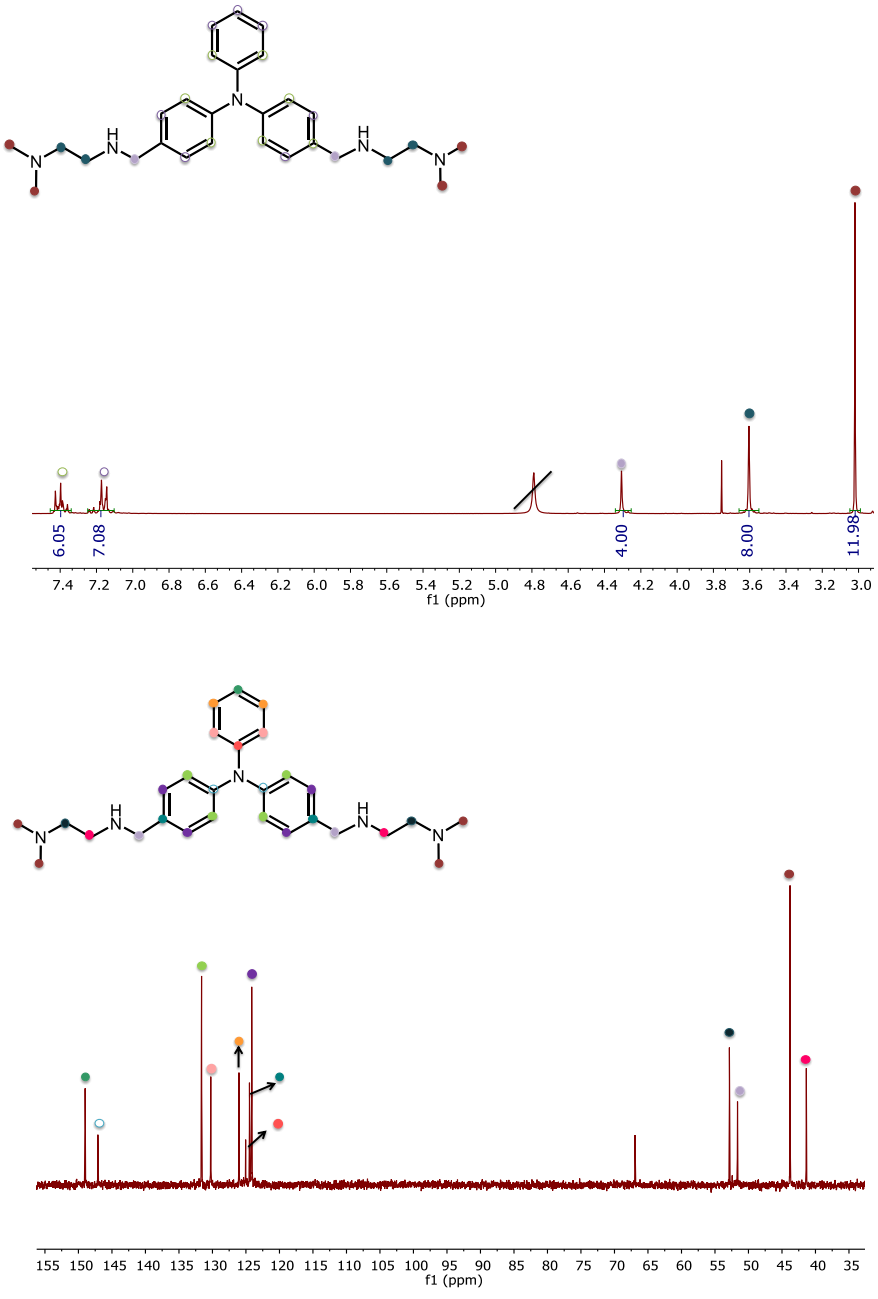

Figure S25. ^{1}H-NMR and ^{13}C-NMR spectra of **TPA2PX** hydrochloride salt in D_2O.

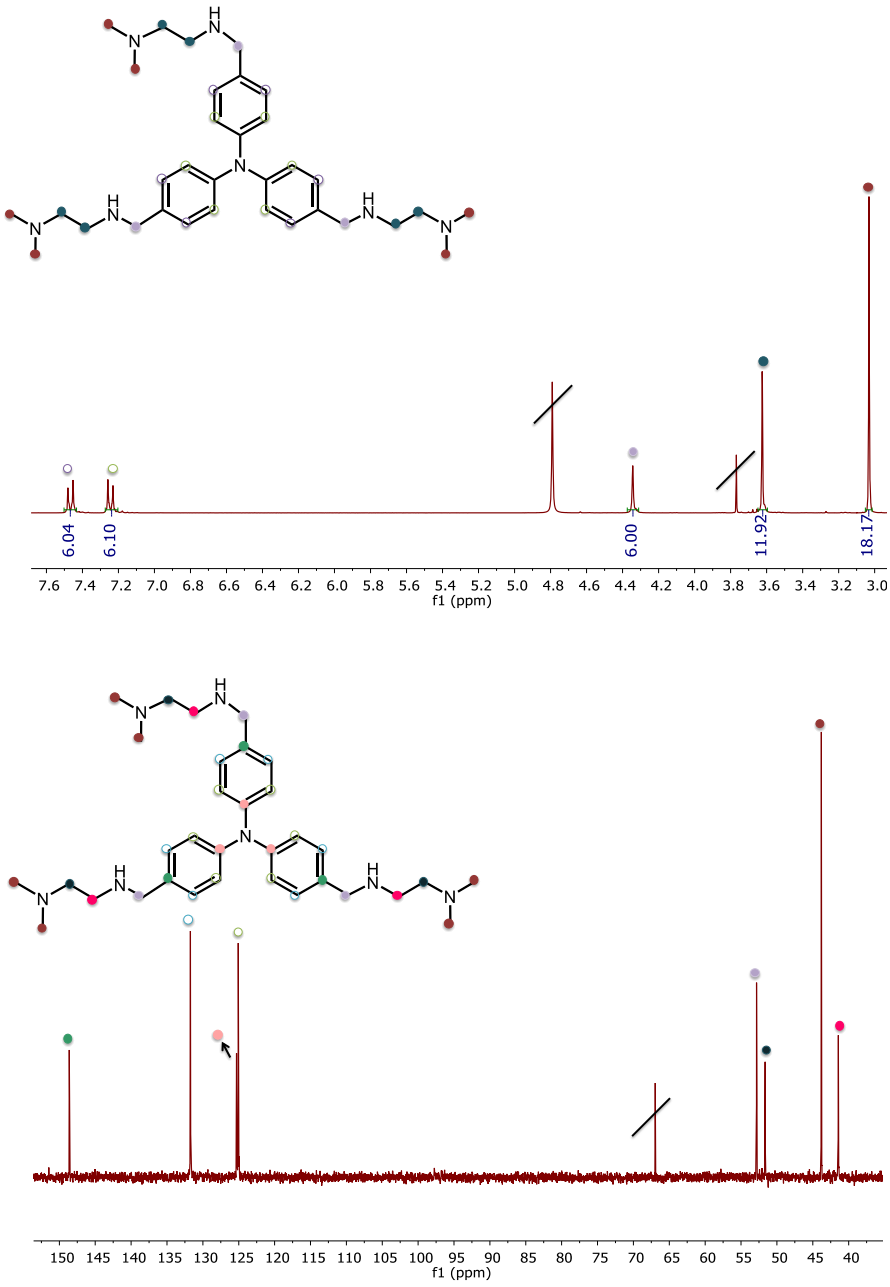

Figure S26. ^{1}H-NMR and ^{13}C-NMR spectra of **TPA3PX** hydrochloride salt in D_2O.

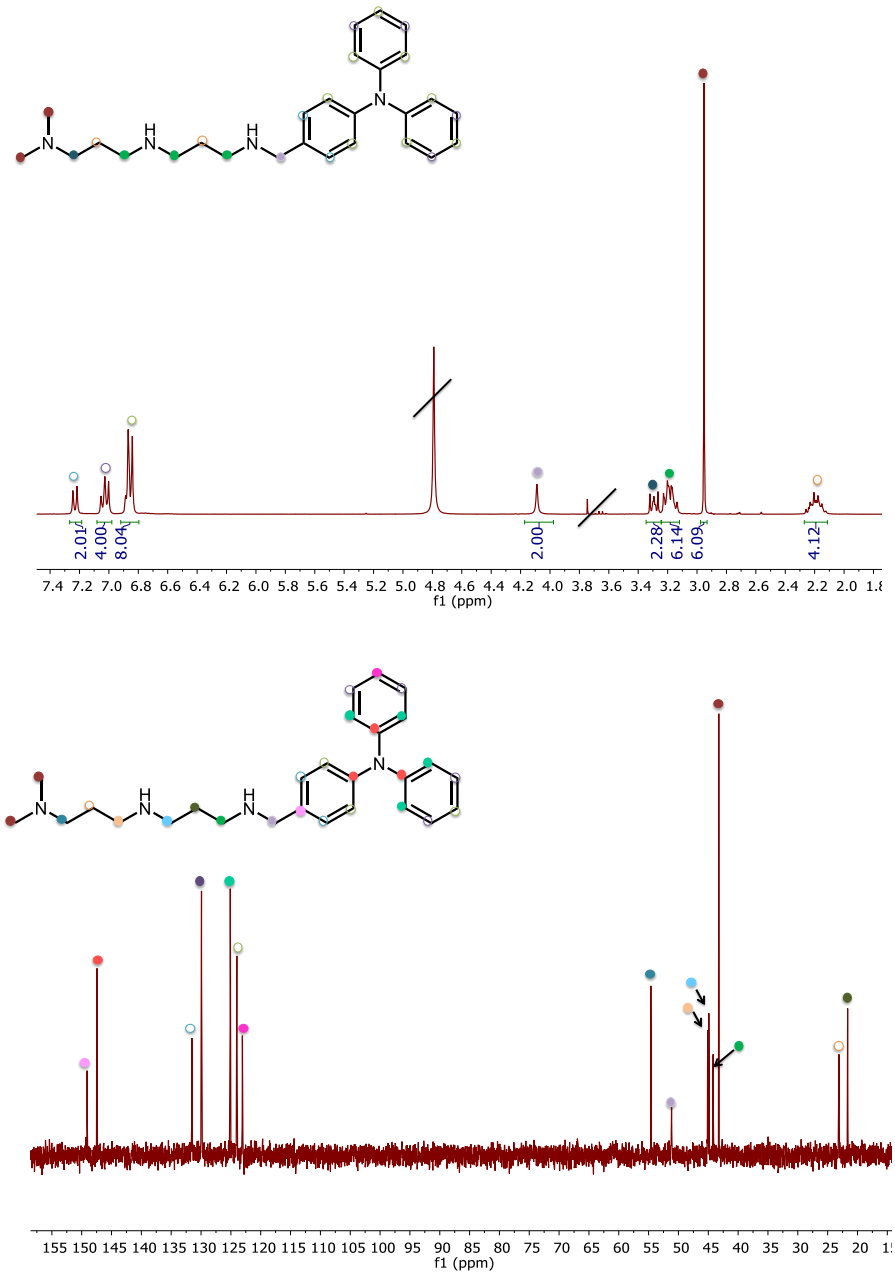

Figure S27. ^{1}H-NMR and ^{13}C-NMR spectra of **TPA1P** hydrochloride salt in D_2O.

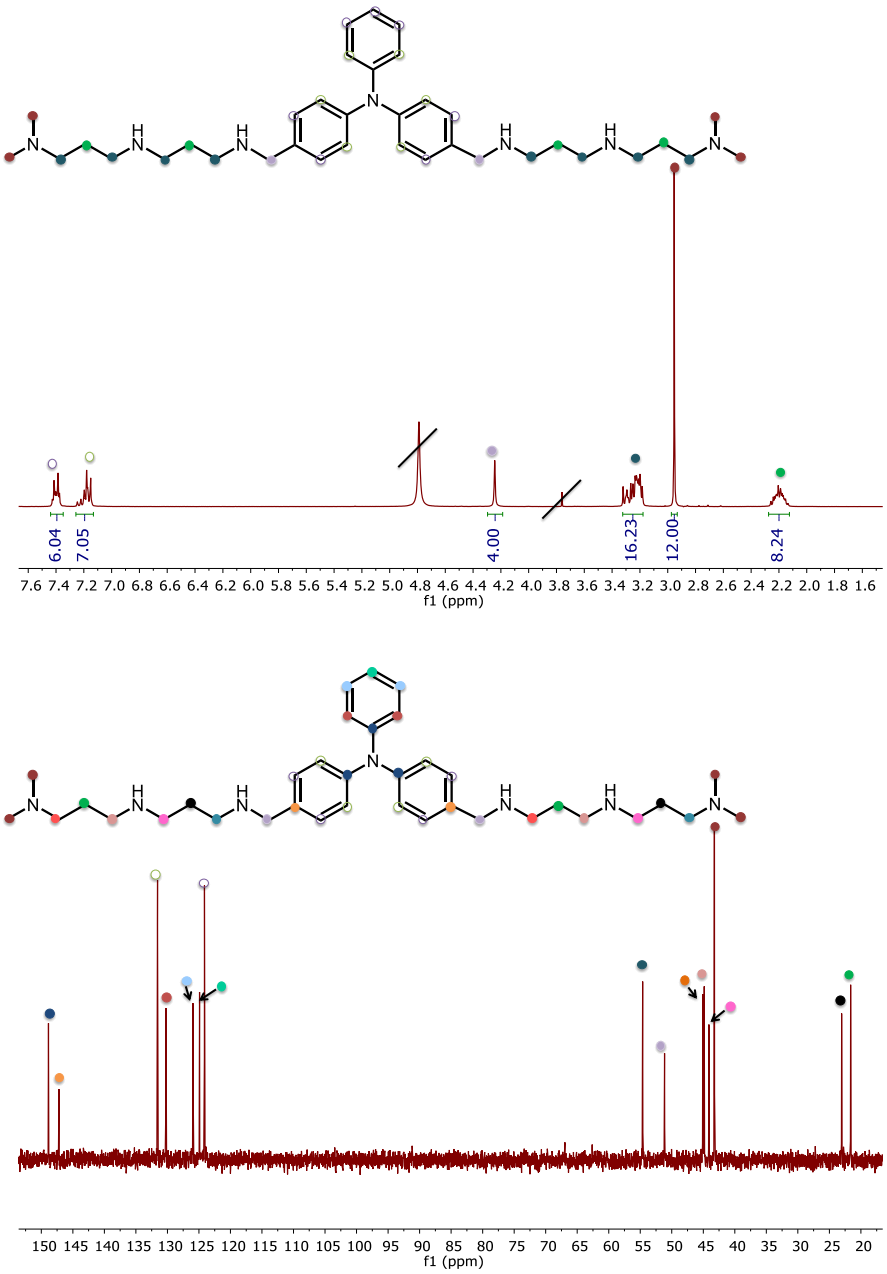

Figure S28. ^{1}H-NMR and ^{13}C-NMR spectra of **TPA2P** hydrochloride salt in D_2O.

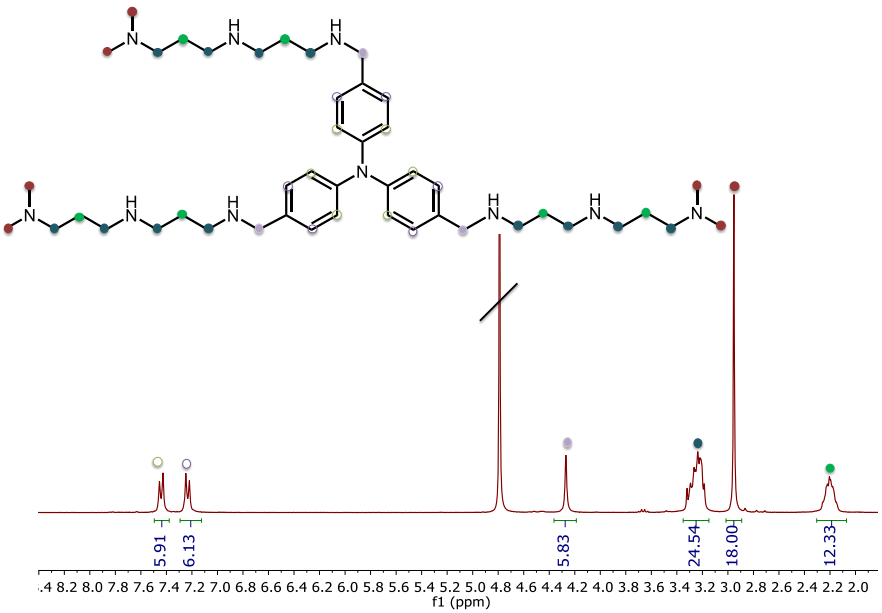

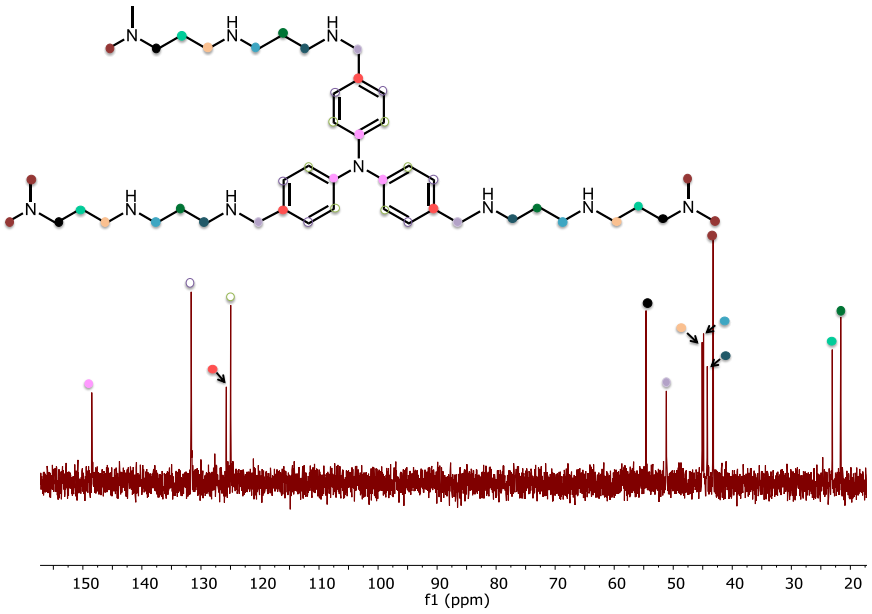

Figure S29. ^{1}H-NMR and ^{13}C-NMR spectra of **TPA3P** hydrochloride salt in D_2O.

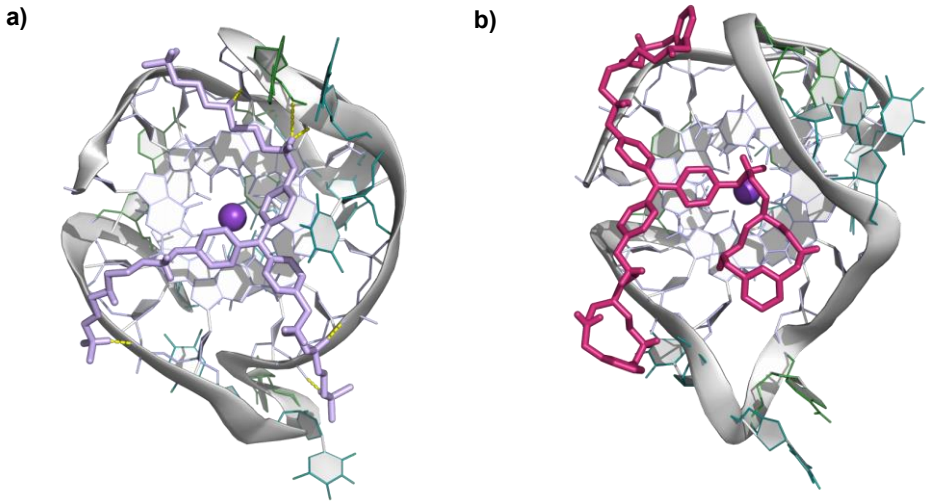

Figure S30. Top view of the minimum energy conformers for de interaction between a) **TPA3P** or b) **TPA3PY** with the G4 DNA model.

Table S.1. Logarithms of the stepwise protonation constants of the three **TPA-PX** ligands determined by potentiometric titrations.[a-c]

Reaction	TPA1PX	TPA2PX	TPA3PX
$H + L \rightleftarrows HL$	8.23(2)	9.16(2)	9.881(7)
$H + HL \rightleftarrows H_2L$	6.28(2)	9.03(1)	9.020(8)
$H + H_2L \rightleftarrows H_3L$		6.60(2)	8.930(6)
$H + H_3L \rightleftarrows H_4L$		5.72(2)	6.86(1)
$H + H_4L \rightleftarrows H_5L$			5.87(1)
$H + H_5L \rightleftarrows H_6L$			5.50(1)
log β	14.51(2)	30.52(2)	46.07(1)

[a] Charges omitted for clarity. [b] Experiments were carried out in a 0.15 M NaCl aqueous solution at 298.1±1 K. [c] Values in parentheses are standard deviations in the last significant figure.

Table S.2. Logarithms of the stepwise protonation constants of the three **TPA-P** ligands determined by potentiometric titrations.[a-c]

Reaction	TPA1P	TPA2P	TPA3P
$H + L \rightleftarrows HL$	8.93(1)	10.268(9)	10.66(2)
$H + HL \rightleftarrows H_2L$	8.874(6)	9.42(5)	10.22(6)
$H + H_2L \rightleftarrows H_3L$	7.327(9)	8.75(2)	9.91(2)
$H + H_3L \rightleftarrows H_4L$		8.61(1)	9.27(1)
$H + H_4L \rightleftarrows H_5L$		7.49(2)	8.76(1)
$H + H_5L \rightleftarrows H_6L$		7.10(2)	8.37(1)
$H + H_6L \rightleftarrows H_7L$			7.77(1)
$H + H_7L \rightleftarrows H_8L$			7.29(1)
$H + H_8L \rightleftarrows H_9L$			6.82(1)
log β	25.132(9)	51.64(2)	78.98(1)

[a] Charges omitted for clarity. [b] Experiments were carried out in a 0.15 M NaCl aqueous solution at 298.1±1 K. [c] Values in parentheses are standard deviations in the last significant figure.

Table S3. ΔT_m values [ºC] for the interaction between different DNA topologies (0.2 μM) and the **TPA-PX** derivatives.

Compound	TPA1PX			TPA2PX			TPA3PX		
Ratio DNA:L	1 :2	1 : 5	1 : 10	1 :2	1 : 5	1 : 10	1 :2	1 : 5	1 : 10
HTelo21-K	8	-2(1)	-2(1)	1(1)	2(2)	4(2)	0(2)	1(1)	5(2)
HTelo21-Na	0(2)	2(1)	4(2)	1(2)	3(2)	4(2)	3(1)	6(2)	6(1)
22CTA	0(2)	0.2(6)	0.3(6)	1.1(8)	2(1)	1(1)	1(1)	2(1)	3(1)
BCl-2	0(1)	0(1)	-0.9(8)	1(1)	1.0(9)	1.0(8)	0(1)	-1(1)	3(1)
c-Myc	2.0(7)	2.5(7)	2.7(9)	1.1(8)	2.0(1)	2.1(8)	1(1)	2(1)	4(1)
CEB25	0.0(6)	0.7(3)	-1.2(4)	-0.3(5)	-0.5(5)	-0.7(5)	-0.5(2)	-0.3(7)	0.5(3)
c-kit1	0(1)	0.3(8)	0.1(8)	0.13(5)	0.7(3)	0.5(2)	0.3(3)	0.2(5)	1.8(6)
c-kit2	2.1(7)	2.1(7)	2.3(9)	1.4(8)	2.0(1)	1.2(1)	1.5(1)	1.9(1)	3(1)
ds26	0.1(2)	0.1(3)	-0.1(2)	0.1(1)	0.1(1)	0.0(3)	0.0(1)	0.0(1)	0.2(1)

Table S4. ΔT_m values [ºC] for the interaction between different DNA topologies (0.2 μM) and the **TPA-P** derivatives.

Compound	TPA1P			TPA2P			TPA3P		
Ratio DNA:L	1 :2	1 : 5	1 : 10	1 :2	1 : 5	1 : 10	1 :2	1 : 5	1 : 10
HTelo21-K	0(2)	3(2)	7(3)	2(2)	8(1)	13(3)	5(3)	18(3)	24(3)
HTelo21-Na	2(1)	8(3)	12(2)	6.1(3)	12.9(3)	17(1)	11(2)	24(6)	33(3)
22CTA	0.2(6)	2(2)	3.7(7)	1.1(3)	5(1)	6.4(9)	4.6(9)	12(1)	22(2)
BCl-2	-1(1)	-2.8(7)	-2.9(6)	-1.5(4)	-1.3(5)	2.6(5)	1.7(8)	14.0(8)	17.7(7)
c-Myc	-0(1)	1.7(8)	5(1)	6(2)	8(2)	10(4)	4(2)	15(3)	25(7)
CEB25	-0.6(4)	-1.1(7)	-1.9(4)	-0.7(7)	-1.6(3)	0.2(2)	-1.2(2)	5.3(4)	10.4(4)
c-kit1	1(2)	2(2)	2.2(7)	1.2(4)	2.6(5)	5.0(5)	3.3(7)	10.7(8)	20.2(8)
c-kit2	0(1)	1.7(8)	5(1)	2(2)	7(3)	10(4)	5(2)	15(3)	25(6)
ds26	0.1(6)	-0.1(6)	-0.3(5)	0.1(4)	0.1(2)	-0.2(3)	-0.1(2)	-0.1(2)	0.5(5)

Table S5. ΔT_m values [ºC] for the interaction between different DNA topologies (0.2 μM) and the **TPA-PY** derivatives.[1]

Compound	TPA1PY			TPA2PY			TPA3PY		
Ratio DNA:L	1 :2	1 : 5	1 : 10	1 :2	1 : 5	1 : 10	1 :2	1 : 5	1 : 10
HTelo21-K	0.2(3)	1.2(2)	3.3(1)	5.7(5)	12.4(2)	20.9(2)	2.9(6)	11.3(7)	18.7(5)
HTelo21-Na	3(1)	0.9(2)	15.5(5)	0.35(8)	16.5(6)	26.7(2)	14(2)	26.6(6)	44.1(8)
22CTA	0.4(4)	0.6(2)	1.0(3)	2.2(5)	7.13(5)	15.4(1)	2.5(5)	7.7(7)	16.8(7)
BCl-2	0.4(1)	0.3(4)	1.6(2)	0.72(9)	3.6(1)	10.54(8)	2.3(2)	7.9(1)	17.2(1)
c-Myc	1.1(3)	0.4(1)	2.4(9)	5.1(3)	10.6(1)	18.01(2)	11.2(5)	20.5(1)	35.4(5)
CEB25	0.1(1)	0.7(9)	0.8(2)	0.12(1)	2.4(3)	7.9(7)	1.5(1)	8.7(1)	15.2(4)
c-kit1	1.3(2)	2(2)	2.2(7)	1.2(4)	2.7(5)	5.0(5)	3.4(7)	10.7(8)	18.2(8)
c-kit2	0.1(1)	0.14(1)	1(1)	2.6(6)	8(2)	10(4)	4.7(1)	14(2)	25.4(6)
ds26	0.2(7)	0.1(2)	0.3(2)	0.01(6)	1.4(2)	4.7(2)	0.36(1)	3.8(2)	14(1)

References

[1] I. Pont, J. González-García, M. Inclán, M. Reynolds, E. Delgado-Pinar, M. T. Albelda, R. Vilar, E. García-España, *Chem. Eur. J.* **2018**, *24*, 10850–10858.